Discrete Breathers in Condensed Matter

S. Flach[1] and Y. Zolotaryuk[2]

[1] Max Planck Institute for the Physics of Complex Systems, Nöthnitzer Str. 38, D-01187 Dresden, Germany
[2] Section for Mathematical Physics, IMM, Technical University of Denmark, Building 321, Richard Petersens Plads, DK-2800 Kgs. Lyngby, Denmark

Abstract. Discrete breathers - non-topological spatially localized time periodic excitations - are generic solutions for lattice Hamiltonians independent of the lattice dimension. We give an introduction to the field including such aspects as spatial tail properties, lattice dimension induced energy thresholds, quantization and experimental applications. We then present recent results on breather properties in spin lattices and Josephson junction ladders. In easy plane ferromagnetic spin lattices the breather states are characterized by a local tilt of the magnetization and nonzero activation energies even in one-dimensional lattices. In Josephson junction ladders breathers lock to the external dc bias current. Variations of the current are used to generate switchings between different breather states and to probe the internal electromagnetic modes of the ladder.

1 Introduction

The study of dynamical non-topological localization in translationary invariant nonlinear Hamiltonian lattices has experienced a considerable development during the past decade [1–3]. The discreteness of space - i.e., the usage of a spatial lattice - is crucial in order to provide structural stability for spatially localized excitations. Spatial discreteness is a very common situation for various applications from, e.g., solid state physics.

To make things precise, let us consider a d-dimensional hypercubic spatial lattice with discrete translational invariance. Each lattice site is labeled by a d-dimensional vector l with integer components. To each lattice site we associate one pair of canonically conjugated coordinates and momenta X_l, P_l which are real functions of time t. Let us then define some Hamiltonian H being a function of all coordinates and momenta and further require that H has the same symmetries as the lattice. The dynamical evolution of the system is given by the usual Hamiltonian equations of motion. Without loss of generality, let us demand that H is a nonnegative function and that $H = 0$ for $X_l = P_l = 0$ (for all l's). We call this state the classical ground state. Generalizations to other lattices and larger numbers of degrees of freedom per lattice site are straightforward.

When linearizing the equations of motion around $H = 0$, we obtain an eigenvalue problem. Due to translational invariance the eigenvectors will be spatially extended plane waves, and the eigenvalues Ω_q (frequencies) form

a phonon spectrum, i.e., Ω_q is a function of the wave vector q. Due to the translation symmetry of the Hamiltonian, Ω_q will be periodic in q. Moreover, the phonon spectrum will be bounded, i.e., $|\Omega_q| \leq \Omega_{max}$. Depending on the presence or absence of Goldstone modes Ω_q might be gapless (zero belongs to the spectrum, spectrum is acoustic) or exhibit a gap ($|\Omega_q| \geq \Omega_{min}$, spectrum is optical). Increasing the number of degrees of freedom per lattice site induces several branches in Ω_q with possible gaps between them.

Let us search for spatially localized time periodic solutions of the full nonlinear equations of motion, i.e., $X_{|l| \to \infty} \to 0$, and

$$X_l(t) = X_l(t + T_b) + \lambda k_l \quad , \quad P_l(t) = P_l(t + T_b) \; , \tag{1}$$

with k_l being integers and λ a spatial period (the equations of motion should be invariant under shifts of X_l by multiples of λ if applicable). These solutions are coined discrete breathers. If $k_l \neq 0$ for a finite subset of lattice sites, the solutions are sometimes coined "rotobreathers".

If a solution exists, we can expand it into a Fourier series in time, i.e., $X_l(t) = \sum_k A_{kl} e^{ik\omega_b t}$ ($\omega_b = 2\pi/T_b$). Spatial localization implies $A_{k,|l| \to \infty} \to 0$. Insert these series into the equations of motion. This results in a set of coupled algebraic equations for the Fourier amplitudes [3]. Consider the spatial tail of the solution where all Fourier amplitudes are small and should further decay to zero with growing distance from the excitation center. Since all amplitudes are small, the equations of motion can be linearized. This procedure decouples the interaction in k-space and we obtain for each k a linear equation for A_{kl} with coupling over l. This equation will contain $k\omega_b$ as a parameter. It will in fact be identical to the above discussed equation linearized around $H = 0$ and it will contain $k\omega_b$ instead of Ω_q [3]. If $k\omega_b = \Omega_q$, the corresponding amplitude A_{kl} will not decay in space, instead it will oscillate. To obtain localization, we arrive at the non-resonance condition [3]

$$k\omega_b \neq \Omega_q \; . \tag{2}$$

This condition has to be fulfilled for all integer k. For an optical spectrum Ω_q, frequency ranges for ω_b exist which satisfy this condition. For acoustic spectra, $k = 0$ poses a problem. We will discuss this case below in more detail.

The non-resonance condition is only a necessary condition for generic occurrence of discrete breathers. More detailed analysis shows that breathers being periodic orbits bifurcate from band edge plane waves [4]. The condition for this bifurcation is an inequality involving parameters of expansion of H around $H = 0$ [4].

Discrete breathers (periodic orbits) appear generically as one-parameter families of periodic orbits. The parameter of the family can be, e.g., the frequency (or energy, action, etc.). Note that we do not need any topological requirement on H (no energy barriers). Indeed, breather families possess limits where the breather delocalizes and its amplitude becomes zero.

With the help of the non-resonance condition we can exclude the generic existence of spatially localized solutions which are quasi-periodic in time. Indeed, in the simplest case we would have to satisfy a non-resonance condition $k_1\omega_1 + k_2\omega_2 \neq \Omega_q$ for ω_1/ω_2 being irrational and all possible pairs of integers k_1, k_2. This is impossible [5].

Note that in many cases breathers can be easily excited by choosing some localized perturbation of the lattice system. Integrating numerically the equations of motion, we find that the energy distribution is not delocalizing, but stays essentially localized over several orders of magnitude of the characteristic phonon periods. These numerical results clearly show that breathers are not only interesting solutions, but can be rather typical and robust depending on the system's parameters.

Note that breathers can exist for autonomous forced damped systems as well [6]. In these systems, contrary to the Hamiltonian ones, breather periodic orbits do not come in one-parameter families of the frequency ω_b, but correspond to limit cycle attractors which are isolated in the system's phase space.

2   Spatial Decay Properties of Discrete Breathers

Consider the Hamiltonian

$$H = \sum_l \left[\frac{1}{2}P_l^2 + V(X_l) + \sum_{l' \neq l} W_{l-l'}(X_l - X_{l'}) \right] \tag{3}$$

with $V(z), W_l(z)$ being nonnegative functions and $V(0) = W_l(0) = 0$. If $\partial^2 V/\partial z^2$ is nonzero for $z = 0$, then Ω_q is optical. In the opposite case, the phonon spectrum is acoustic. If Ω_q is optical and Ω_q^2 an analytical function in q (this is realized for any finite range interaction $W_{l>l_c} = 0$, but also, e.g., for $W_l(z)$ exponentially decaying in l), the interaction part of H is called short-ranged. To compute the spatial decay of a breather solution, we use the above mentioned linearized equations for its Fourier amplitudes A_{kl}. With the help of Green's function method we find that [7]

$$A_{kl} \sim \int_\Xi \frac{\cos(ql)}{(k\omega_b)^2 - \Omega_q^2} \mathrm{d}^d q \ . \tag{4}$$

Here the integration extends over Ξ - the first Brillouin zone. Due to general properties of convergence of Fourier series [8] we conclude that for short-range interactions A_{kl} decay exponentially in l, where the exponents depend on k [5]. The exponent of A_{kl} tends to zero whenever $k\omega_b$ approaches an edge of Ω_q. Note that in such a limit the linearization of the algebraic equations in the tails of the breather ceases to be correct for a finite number of selected $k' \neq k$ and nonlinear corrections to (4) apply (see [9]). Still, the spatial decay is exponential.

2.1   Algebraically Decaying Interactions

Consider a one-dimensional lattice with algebraically decaying interactions $W_l(z) \sim 1/l^s$ and $\partial^2 V/\partial z^2|_{z=0} \neq 0$. Since Ω_q^2 is non-analytical in q, for this case, (4) implies that for large distances l the spatial decay of a breather will be algebraic [7]: $A_{kl} \sim 1/l^s$. However, for $s \to \infty$ the spatial decay becomes short-ranged (nearest-neighbor interactions). To understand the crossover to exponential decay in this limit, consider (4) for the case when $k\omega_b$ is very close to the edge of Ω_q which is characterized by some wave vector q_c. Since the integrand nearly diverges near q_c, we may use a stationary phase approximation and expand Ω_q^2 around q_c taking into account only the leading order term. For $s > 3$ the leading order dependence of Ω_q^2 on q will be proportional to $(q - q_c)^2$. The non-analytic behavior is then hidden in higher order terms in $(q - q_c)$ and does not contribute within the approximation [7]. Since we approximate Ω_q^2 by an analytical function, we will obtain exponential decay in space. However, we know that the asymptotic dependence of A_{kl} on l is algebraic. We thus conclude that in the mentioned case of $k\omega_b$ being close to the edge of Ω_q, the spatial decay will be exponential for intermediate distances, but becomes algebraic for distances larger than some crossover distance l_c. High-precision numerical computations confirm this prediction [7]. The crossover distance can be estimated as

$$\frac{\ln l_c}{l_c} \approx \frac{\nu}{s} \tag{5}$$

where ν is the exponent of the spatial decay obtained within the stationary phase approximation [7]. It follows from the result (5) that $l_c \to \infty$ as $s \to \infty$. This is an expected result, since in this short-range interaction limit we recover exponential decay in the whole space. More surprising is also that the limit $\nu \to 0$ (i.e. $k\omega_b \to \Omega_{q_c}$) yields $l_c \to \infty$. The exponential decay is thus also obtained in the whole space whenever the frequency (or its multiple) of the breather solution comes close to the edge of Ω_q.

2.2   Presence of Goldstone Modes - Acoustic Breathers

When Ω_q contains zero, i.e., when the linearized equations around $H = 0$ contain Golstone modes as solutions, the dc component of a breather solution A_{kl} with $k = 0$ deserves special attention. All ac components ($k \neq 0$) can be analyzed similar to the case of an optical spectrum. If the Hamiltonian is invariant under the transformation $X_l \to -X_l$, then time-periodic solutions being invariant under this transformation will have $A_{kl} = 0$ for even k which includes $k = 0$. However if such a parity symmetry is broken, all the Fourier components become nonzero.

Assume that Ω_q^2 is analytical in q. Since the $k = 0$ component cannot decay exponentially in space, at large distances from the breather, the leading order part of the solution will be given by its slowly decaying dc part, the

static lattice distortion. Its corresponding linearized equation will be similar to the equation for a strain in continuum mechanics, which is induced by some local deformation (the breather center) of the system [10]. The strain will decay algebraically in space. The constraint of finite energies leads to the requirement that the monopole contribution to the local deformation is zero for $d = 1, 2$. The resulting algebraic decay $A_{0l} \sim 1/|l|^{d-1}$ induced by a dipole has been confirmed numerically for $d = 2$ [10].

3   Energy Thresholds for Discrete Breathers

A direct consequence of the spatial decay properties of discrete breathers is the possible appearance of nonzero energy thresholds. We remind that breathers show up as one-parameter families of time-periodic solutions in phase space. When sliding along such a family, all the parameters characterizing the breather continuously change. The presence or absence of an energy gap is of physical importance. First we observe that the only limit, where the breather energy could vanish, is the limit of zero amplitudes, i.e., the limit when ω_b approaches the edge of Ω_q. Let us estimate the far field energy part of a breather E_b,

$$E_b \sim \int_1^\infty r^{d-1} F_d^2(\delta r) \mathrm{d}r \tag{6}$$

where the energy density is proportional to $A_{1r}^2 \sim F_d^2(\delta r)$. Since in the considered limit the spatial decay is weakly exponential (no matter whether Ω_q^2 is analytical or not), the function $F_d(\delta r)$ is bounded by an exponential function with exponent δ. Assuming that the dispersion near the band edge in Ω_q is in the leading order quadratic in $(q - q_c)$, we find $\delta \sim |\omega_b - \Omega_{q_c}|$. In the same limit, using the perturbation theory for weakly nonlinear plane waves with amplitude A and frequency ω_b, we can estimate $|\omega_b - \Omega_{q_c}| \sim A^2$. Since the breather in the considered limit is a slightly distorted (localized) plane wave, we finally arrive at [11]

$$E_b \sim |\omega_b - \Omega_{q_c}|^{1-d/2} \quad . \tag{7}$$

This result implies that the breather energy cannot assume arbitrary small values for $d \geq 2$. Consequently, in such a case, breathers have nonzero lower bounds on their energy (and similarly on their action). In some special cases, nonzero energy gaps may occur even for one-dimensional systems [11]. Also, non-analytical dispersion Ω_q^2 may lower the critical lattice dimension [7].

4   Quantization and Applications

Quantizing the actions on a given family of classical breather solutions will select a set of eigenenergies. However, each of them will be highly degenerated,

with a multiplicity of at least the number of sites in the lattice. We expect that these degeneracies will be lifted. The corresponding band width may be responsible for a finite probability of breather tunneling [12]. In other words, the expectation is that the quantum analogues of classical breathers are many phonon bound states. Numerical studies on lattices are severely restricted by the number of states per lattice site and the number of lattice sites. So far, the studies on six sites have been done with a restriction to the low energy domain of two phonon bound states [13]. Another way of approaching the problem is to study small systems with two or three sites where the tunneling of energy from an excited bond to a non-excited one is considered [14].

The discrete breather concept has been recently used for different experimental situations. Light injected into a narrow waveguide which is weakly coupled to parallel waveguides (characteristic diameter and distances of order of micrometers, nonlinear optical medium based on GaAs materials) disperses to the neighboring channels for small field intensities, but localizes in the initially injected wave guide for large field intensities [15].

Bound phonon states (up to seven participating phonons) have been observed by overtone resonance Raman spectroscopy in PtCl mixed valence metal compounds [16]. The bound states are quantum versions of classical discrete breather solutions.

Spatially localized voltage drops in Nb-based Josephson junction ladders have been recently observed and characterized [17] (typical size of junction is a few micrometers). These states correspond to generalizations of discrete breathers to dissipative systems.

5   Breathers in Classical Spin Lattices

Due to spatial periodicity, lattices of interacting spins are ideal systems to observe discrete breathers as well. Here, we will focus on large spins, which may be described classically. Consider a ferromagnetic lattice of classical spins with the Hamiltonian containing the Heisenberg XYZ exchange interaction and single-ion anisotropy:

$$H = -\frac{1}{2} \sum_{l \neq l'} \sum_{\alpha=(x,y,z)} J_\alpha^{ll'} S_l^\alpha S_{l'}^\alpha - D \sum_l S_l^{z\,2} \ , \tag{8}$$

with S_l^x, S_l^y, S_l^z being the lth spin components which satisfy the normalisation condition $S_l^{x\,2} + S_l^{y\,2} + S_l^{z\,2} = 1$ (l labels lattice sites). The constants $J_x, J_y, J_z > 0$ are the exchange integrals and D is the on-site anisotropy constant. The equations of motion for the spin components in the 1D ferromagnetic spin chain with nearest-neighbor interactions are the well known Landau-Lifshitz equations:

$$\dot{S}_l = -S_l \times \nabla_{S_l} H \ . \tag{9}$$

Three cases will be discussed below: (i) strongly anisotropic exchange $J_x \neq J_y \ll J_z$; (ii) isotropic exchange ($J_x = J_y = J_z \equiv J$) and strong single-ion anisotropy of the easy axis type - $D > 0$; (iii) isotropic exchange and strong easy plane anisotropy - $D < 0$. The ground states of the spin lattices for cases (i) and (ii) are identical - $S_l^z = 1$ or $S_l^z = -1$ for all sites, while the ground state for (iii) is continuously degenerate and corresponds to all spins lying in the easy plane XY and being parallel to each other.

The dispersion relations for small amplitude excitations above the classical ground state for cases (i) and (ii) are similar to each other (Fig. 1a) and they are characterized by a gap. It has been shown in [20] that the
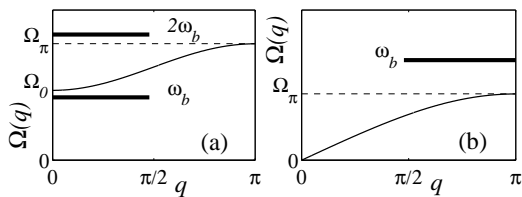

Fig. 1. Dispersion laws for (a) easy-axis and (b) easy-plane ferromagnets. Thick lines indicate possible locations of breather frequencies and their harmonics.

frequency of a discrete breather is located in the gap of Ω_q. For the case (iii) the plane wave spectrum is acoustic (gapless) (see Fig. 1b) and discrete breathers should have frequencies located above the spectrum. A rigorous proof of the existence of discrete breathers based on the implementation of the anti-continuous (AC) limit (see [2,19]) is given in [20].

5.1 Easy axis anisotropy

In the particular case of strong exchange anisotropy, the AC limit has been implemented by setting $J_{x,y} = 0$ and using the coding sequence $\sigma = (...01110...)$ (here $\sigma_l = 1$ means that the lth spin is turned out of its ground state position). In the case of isotropic exchange and on-site anisotropy $D > 0$, we may choose $\sigma = (...010...)$ and $J = 0$. Breathers in these types of lattices can be viewed as localized spin excitations with spins precessing around one of the ground states of the system (e.g., $S^z = 1$), so that the effective radius of this precession decreases to zero as $l \to \pm\infty$ (for more details on this type of breathers see [21]).

If the exchange is isotropic in XY - $J_x = J_y$ - the spin component S_l^z is conserved on the solution, and therefore the separation of the time and space variables is possible: $S_l^{\pm} = S_l^x \pm iS_l^y = A_l \exp(\pm i\omega_b t)$. This implies that the Fourier series expansion of a breather periodic orbit with respect to time consists of only one term. Contrary, for $J_x \neq J_y$ the S_l^z-component is not conserved on the solution and the spin dynamics is not anymore given by a precession around the Z-axis only. At the same time higher order terms appear in the above mentioned Fourier series expansion. Consequently, for

such a case of broken symmetry in the XY plane, breathers do not persist in the limit of large exchange (continuum limit). The reason is that the spectrum Ω_q in this limit still has a gap, but it is unbounded from above. Consequently, there will be unavoidable resonances of higher harmonics of the breather with Ω_q.

5.2   Easy plane anisotropy

The ground state of the lattice, without loss of generality, can be assumed to be $S_l^x = 1, S_l^y = S_l^z = 0$ for all l's. The implementation of the AC limit can be achieved by setting $J = 0$ and exciting one or several spins, so that they should start to precess around the hard axis with a frequency $\omega_b = 2|D|S^z$. For non-zero J, initially non-excited spins start to precess with small amplitudes around the X-axis, while the plane of precession of the "out-of-plane" spin is no longer parallel to the easy plane, being slightly tilted, as shown in Fig. 2. When the breather frequency approaches the upper edge of
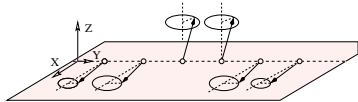

Fig. 2. Schematic representation of the discrete breather with two parallel out-of-plane spins in an easy plane ferromagnet.

Ω_q at $q = \pi$, the breather becomes less localized. Surprisingly, this does not qualitatively influence its core structure, i.e., the effective precessing axis of out-of-plane central spin(s) is not continuously tilted towards the X-axis in this limit. The central spin dynamics can be viewed as periodic (closed) orbits of a point confined to the unit sphere. Let the XY plane be an equatorial one. Then, for large breather frequencies, the point performs small circles around the north (or south) pole. When lowering the breather frequency, the loop still encircles the Z-axis. Thus, the breather solution does not deform into a slightly perturbed and weakly localized excitation above the ground state. Again, we conclude that such breather states do not persist in corresponding continuum theories.

Moreover, we have investigated the dependence of the breather energy on the breather frequency (see Fig. 3). We observe an energy threshold, since the breather energy attains a non-zero minimum, when its frequency is still not equal to the edge of the linear spin wave spectrum. This result being independent of the spin lattice dimension differs from the results of Sec. 3. The reason for the appearance of a non-zero lower bound is hidden in the topology of the central spin dynamics - the central spins are always precessing around the Z-axis, no matter what their frequency is. Therefore the breather cannot be deformed into a perturbed band edge linear wave, which was a key ingredient of the argumentation in Sec. 3.

If we consider the opposite limit of increasing frequency, we find a decrease of the precession radius of the central spin(s). In the AC limit, the upper
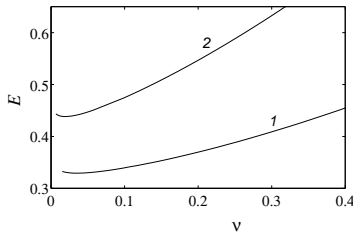
Fig. 3. Normalized energy $E = H + JN/2$ as a function of the detuning frequency $\nu = \omega_b - \Omega(\pi) = \omega_b - \sqrt{4J(|D| + J)}$ for a discrete breather with one out-of-plane spin (curve 1) and with two out-of-plane spins (curve 2) for $J = 0.1$. The size of the system is $N = 30$ spins. For $N = 50$, spins the curves do not differ significantly.

bound for the breather frequency is determined by $\omega = 2D$ which corresponds to the central (precessing) spin(s) being parallel to the Z-axis. This bound continues to exist when the exchange is switched on. After reaching this frequency threshold, the breather becomes a stationary (time-independent) solution.

6 Breathers in Josephson Junction Ladders

Arrays of Josephson junctions are a perfect laboratory object to study various nonlinear phenomena. An anisotropic ladder of dc-biased Josephson junctions as shown in Fig. 4 is perhaps the simplest structure which supports discrete breathers. The dynamics of a single Josephson junction is described by the
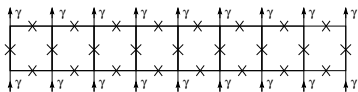

Fig. 4. A schematic view of the Josephson junction ladder. Crosses indicate the locations of junctions, the arrows show the direction of external current flow γ.

time evolution of the difference of the phases of the wave function between adjacent superconducting islands. It may support two stable states: a superconducting state and a resistive state.

6.1 The model and equations of motion

Denote by $\phi_l^v, \phi_l^h, \tilde{\phi}_l^h$ the phase differences across the lth vertical junction and its right upper and lower horizontal neighbors. Then the dimensionless equations of motion for each junction with current I_l, flowing through it, are given by the Josephson equation on its phase difference ϕ_l:

$$\ddot{\phi}_l + \alpha\dot{\phi}_l + \sin\phi_l = I_l \ . \tag{10}$$

The time is normalized to $t_0 = \sqrt{C\Phi_0/(2\pi I_c)}$ with Φ_0 being a magnetic flux quantum, C the capacitance and I_c the critical current of the corresponding junction. The dimensionless damping parameter is $\alpha = \sqrt{\Phi_0/(2\pi I_c C R_N^2)}$ (R_N is the junction resistance) and $\eta = I_{cH}/I_{cV}$ is the anisotropy constant -

the ratio of the critical horizontal and vertical currents. Using the Kirchhof laws and the self-inductance relation for one elementary cell of the ladder (see [18]), one arrives at the following set of equations:

$$\ddot{\phi}_l^v + \alpha\dot{\phi}_l^v + \sin\phi_l^v = \gamma + (\Delta\phi_l^v - \nabla\tilde{\phi}_{l-1}^h + \nabla\phi_{l-1}^h)/\beta_L \ ,$$
$$\ddot{\phi}_l^h + \alpha\dot{\phi}_l^h + \sin\phi_l^h = -(\phi_l^h - \tilde{\phi}_l^h + \nabla\phi_l^v)/(\eta\beta_L) \ , \qquad (11)$$
$$\ddot{\tilde{\phi}}_l^h + \alpha\dot{\tilde{\phi}}_l^h + \sin\tilde{\phi}_l^h = (\phi_l^h - \tilde{\phi}_l^h + \nabla\phi_l^v)/(\eta\beta_L) \ ,$$
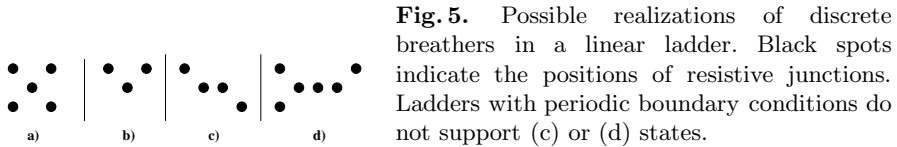
where γ is the dimensionless dc bias in units of I_{cV}, $\beta_L = 2\pi L I_{cV}/\Phi_0$ the dimensionless discreteness parameter and L the self-inductance of the elementary cell of the ladder. The discrete operators are given by $\nabla\phi_l = \phi_{l+1} - \phi_l$, $\Delta\phi_l = \phi_{l+1} - 2\phi_l + \phi_{l-1}$. The dispersion law for the plasmons for the weakly damped case ($\alpha \ll 1$) can be obtained by linearizing the system (11):

$$\Omega_0^2 = 1 \ , \ \Omega_\pm^2 = \left[1 + \xi \pm \sqrt{(1-\xi)^2 + 8(1 - \sqrt{1-\gamma^2})/(\eta\beta_L)}\right]/2 \ , \quad (12)$$

where $\xi = \sqrt{1-\gamma^2} + 2[1 + \eta(1-\cos q)]/(\eta\beta_L)$. The branch Ω_0 corresponds to non-active vertical junctions and in-phase (symmetric) oscillations of the phases of upper and lower horizontal junctions. The branch $\Omega_+ > \Omega_0$ is characterized by anti-symmetric oscillations of the horizontal phases for all q's. For $q = 0$ only the horizontal junctions are excited. The branch $\Omega_- < \Omega_0$ becomes dispersionless for $\gamma = 0$. For $q = 0$ it corresponds to only the vertical junctions being excited, while the horizontal ones are not active.

6.2   Rotobreather solutions and their current-voltage dependencies

The breather states (rotobreathers in this case) correspond to a few junctions being in the resistive state [$k_l \neq 0$ in (1)] with all other junctions oscillating around the superconducting state ($k_l = 0$). Experiments [17] have revealed different breather structures, as depicted in Fig. 5: (a) up-down symmetry, (b)

Fig. 5. Possible realizations of discrete breathers in a linear ladder. Black spots indicate the positions of resistive junctions. Ladders with periodic boundary conditions do not support (c) or (d) states.

left-right symmetry, (c) inversion symmetry, (d) no symmetry. Each group of breathers can also have an arbitrary number n_r of vertical resistive junctions.

Experimentally, each discrete breather is characterized by its current-voltage dependence (see Fig. 6). The average voltage drop on the lth vertical
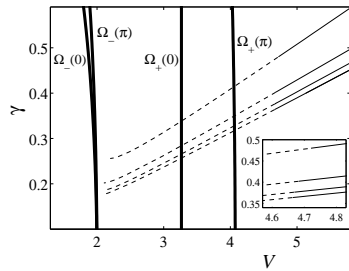
Fig. 6. Current-voltage dependence for breathers of type (a) in an annular ladder of N=30 vertical Josephson junctions with $n_r = 1, 2, 3, 4$ (from top to bottom). The system parameters are: $\alpha = 0.07$, $\eta = 0.44$, $\beta_L = 2.7$. Dashed lines correspond to unstable breathers. The thick lines correspond to the γ-dependent band edges of $\Omega_\pm(q)$.

junction equals $V = (1/T_b) \int_0^{T_b} \dot{\phi}_l^v dt$. For type (a,d) breathers $V = 2\omega_b$ and for type (b,c) ones $V = \omega_b$.

The stability of rotobreather solutions has been studied by diagonalizing the corresponding monodromy (Floquet) matrix (see Fig. 7). The figure
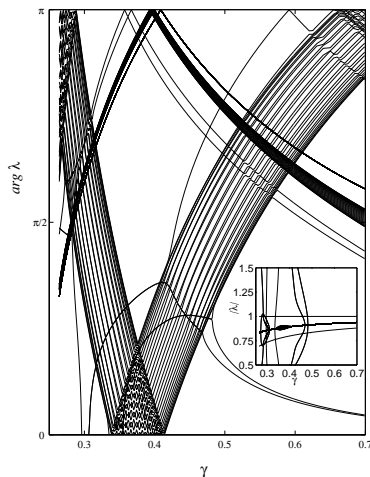

Fig. 7. Dynamics of the eigenvalues λ of the monodromy (Floquet) matrix for the top current-voltage line of Fig. 6 ($n_r = 1$). The monodromy matrix is obtained by linearizing the phase space flow around a breather periodic orbit: $\phi_n(t) = \phi_n^{(b)}(t) + \epsilon_n(t)$ and computing the map

$$\begin{bmatrix} \epsilon_n(T) \\ \dot{\epsilon}_n(T) \end{bmatrix} = \hat{\mathcal{M}} \begin{bmatrix} \epsilon_n(0) \\ \dot{\epsilon}_n(0) \end{bmatrix} .$$

Stability of the breather solution is given only if all Floquet eigenvalues reside inside the unit circle.

reveals an important collision of Floquet eigenvalues around $\gamma \approx 0.5$. As a result, one of the eigenvalues crosses the unit circle upon further current decrease at $\gamma \approx 0.45$ (see the inset). The eigenvalues which participate in the collision correspond to a Floquet mode localized around the breather and the other one which corresponds to the delocalized Ω_+ branch of the plane wave spectrum. This scenario can be translated into a combination resonance criterion when the breather frequency mediates some resonant interaction between the two Floquet modes - a localized and a delocalized one [18].

7   Instead of a Conclusion

Discrete breathers are generic solutions of nonlinear lattice equations, they are localized in space and periodic in time. Their existence is *not* confined to certain lattice dimensions. The necessary existence condition for discrete breathers is the absence of resonances of all multiples of the breather frequency with the linear plane wave spectrum of the system. Spin lattices and arrays of Josephson junctions, which have been discussed above, are not the only systems which support discrete breathers. Other applications include polaron (Davydov's soliton) formation in biomolecules (see [22,23]), diluted Bose-Einstein condensates [24], light localization in weakly coupled optical waveguides [15], many phonon bound states in solids [16], to name a few.

References

1. A. J. Sievers and J. B. Page: in *Dynamical Properties of Solids VII Phonon Physics The Cutting Edge*, ed. G. K. Horton and A. A. Maradudin (Elsevier, Amsterdam 1995).
2. S. Aubry: Physica D **103**, 201 (1997).
3. S. Flach and C. R. Willis: Phys. Rep. **295**, 182 (1998).
4. S. Flach: Physica D **91**, 223 (1996).
5. S. Flach: Phys. Rev. E **50**, 3134 (1994).
6. R. S. MacKay and J. A. Sepulchre: Physica D **119**, 148 (1998).
7. S. Flach: Phys. Rev. E **58**, R4116 (1998).
8. A. Zygmund: *Trigonometric Series* (Cambridge University, Cambridge 1963).
9. S. Flach: Phys. Rev. E **51**, 3579 (1995).
10. S. Flach, K. Kladko, and S. Takeno: Phys. Rev. Lett. **79**, 4838 (1997).
11. S. Flach, K. Kladko, and R. S. MacKay: Phys. Rev. Lett. **78**, 1207 (1997).
12. V. Fleurov, R. Schilling and S. Flach: Phys. Rev. E **58**, 339 (1998).
13. W. Z. Wang et al: Phys. Rev. Lett. **80**, 3284 (1998).
14. S. Aubry et al: Phys. Rev. Lett. **76**, 1607 (1996); S. Flach and V. Fleurov: J. Phys.: Cond. Mat. **9**, 7039 (1997); S. Flach, V. Fleurov, and A. A. Ovchinnikov: Phys. Rev. B **63**, 094304 (2001).
15. H. S. Eisenberg et al: Phys. Rev. Lett. **81**, 3383 (1998).
16. B. I. Swanson et al: Phys. Rev. Lett. **82**, 3288 (1999).
17. P. Binder et al: Phys. Rev. Lett. **84**, 745 (2000); E. Trias, J. J. Mazo and T. P. Orlando: Phys. Rev. Lett. **84**, 741 (2000); P. Binder, D. Abraimov, and A. V. Ustinov: Phys. Rev. E **62**, 2858 (2000).
18. A. E. Miroshnichenko et al: cond-mat/0103280.
19. R. S. MacKay and S. Aubry: Nonlinearity **7**, 1623 (1994).
20. Y. Zolotaryuk, S. Flach, and V. Fleurov: to appear in Phys. Rev. B (2001), cond-mat/0009218.
21. R. Lai and A. J. Sievers: Phys. Rep. **314**, 147 (1999).
22. A. C. Scott: Phys. Rep. **217**, 1 (1992).
23. A. Xie et al: Phys. Rev. Lett. **84**, 5435 (2000).
24. A. Trombettoni and A. Smerzi: Phys. Rev. Lett. **86**, 2353 (2001).